Neuron, Volume *102*

Supplemental Information

Multimodal Single-Cell Analysis Reveals Physiological Maturation in the Developing Human Neocortex

Simone Mayer, Jiadong Chen, Dmitry Velmeshev, Andreas Mayer, Ugomma C. Eze, Aparna Bhaduri, Carlos E. Cunha, Diane Jung, Arpana Arjun, Emmy Li, Beatriz Alvarado, Shaohui Wang, Nils Lovegren, Michael L. Gonzales, Lukasz Szpankowski, Anne Leyrat, Jay A.A. West, Georgia Panagiotakos, Arturo Alvarez-Buylla, Mercedes F. Paredes, Tomasz J. Nowakowski, Alex A. Pollen, and Arnold R. Kriegstein

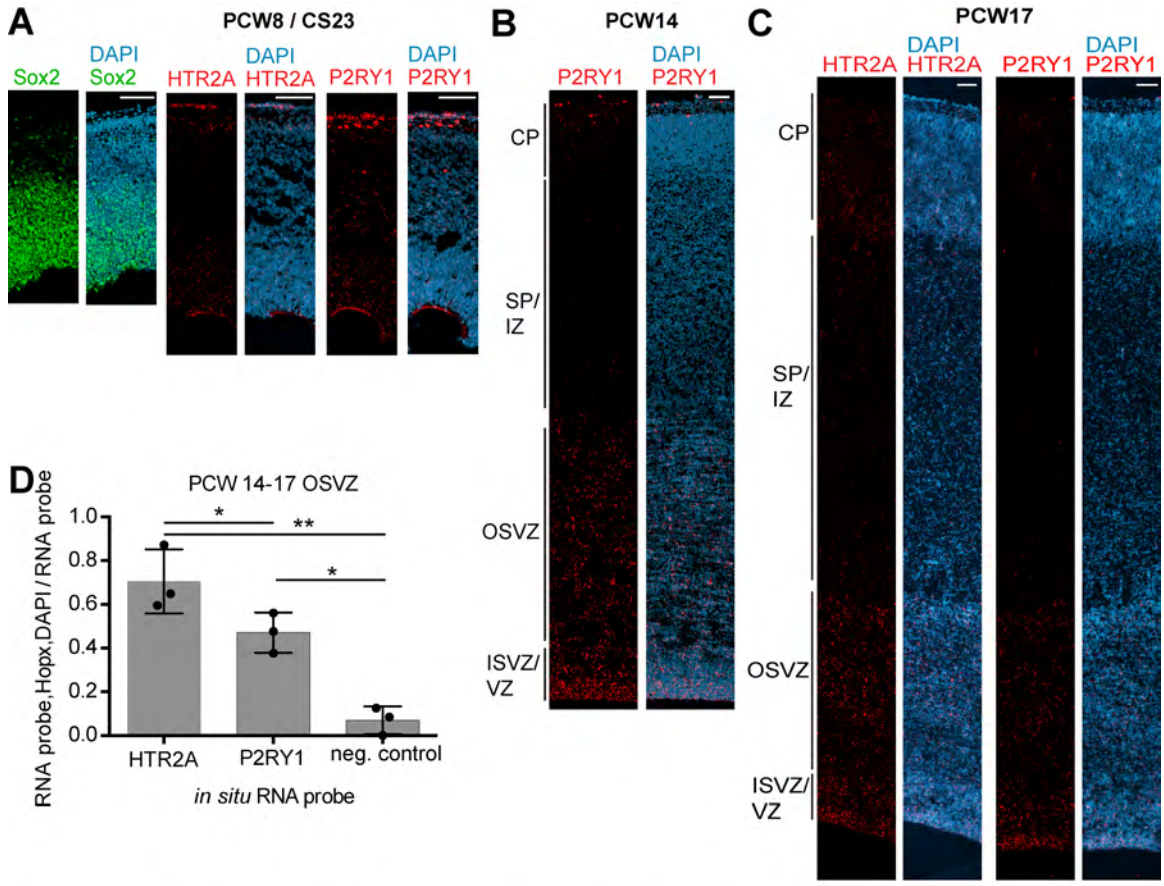

E **Htr2a expression appears postnatally in the developing mouse neocortex**

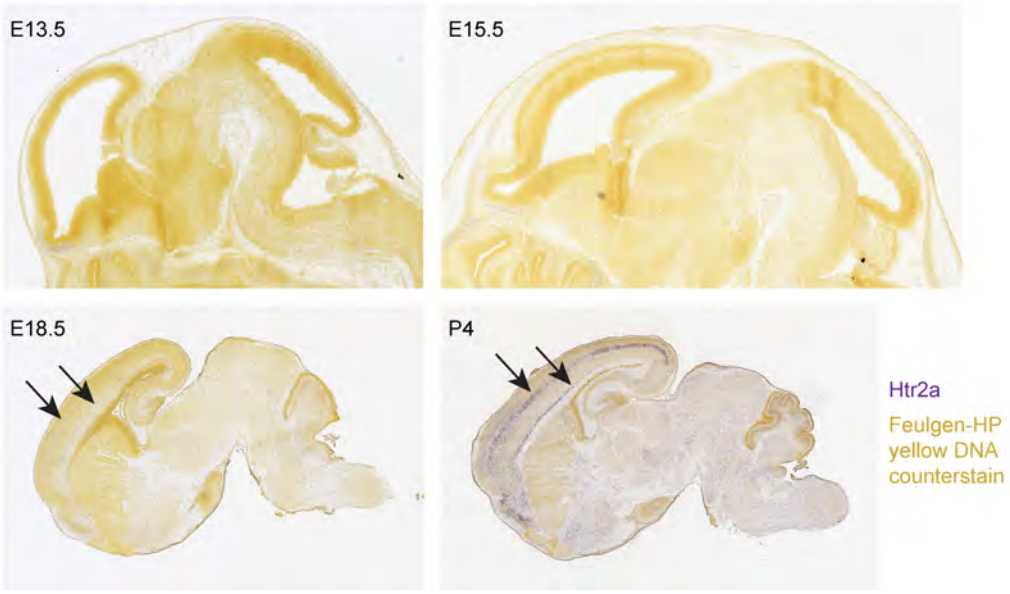

Figure S1 Spatiotemporal expression of *HTR2A* and *P2RY1* in the developing human and mouse neocortex, Related to Figure 1: (A) Immunohistochemistry for Sox2 shows the progenitor zone in the developing human neocortex at PCW8 (left). Single molecule *in situ* hybridization for *HTR2A* and *P2RY1* in adjacent sections (middle, right) together with DAPI staining. **(B)** Single molecule *in situ* hybridization for *P2RY1* in PCW14 cortical section together with DAPI. See Figure1F for comparison with *HTR2A* expression at this age. **(C)** Single molecule *in situ* hybridization for *HTR2A* and *P2RY1* in PCW17 cortical section together with DAPI. Tile scans show cross-sections of the developing neocortex. (A-C) Scale bar: 100 µm. Images were adjusted for tonality and brightness. Tile scan shows cross-section of the developing neocortex showing the ventricular and inner subventricular zone (VZ/ISVZ), the outer subventricular zone (OSVZ), subplate and intermediate zone (SP/IZ), and the cortical plate (CP). **(D)** Quantification of colocalization of RNAscope puncta (*HTR2A*, *P2RY1* and negative control probe) with areas immunopositive for the outer radial glia cell marker HOPX in the outer subventricular zone (OSVZ). Data are represented as mean ± SEM. * $p<0.05$, ** $p<0.01$, dots indicate biological replicates **(E)** *In situ* hybridization for Htr2A in the developing mouse brain. Note expression of Htr2a starts at E18.5 in the neocortex. Source: Allen Developing Mouse Brain Atlas (2008).

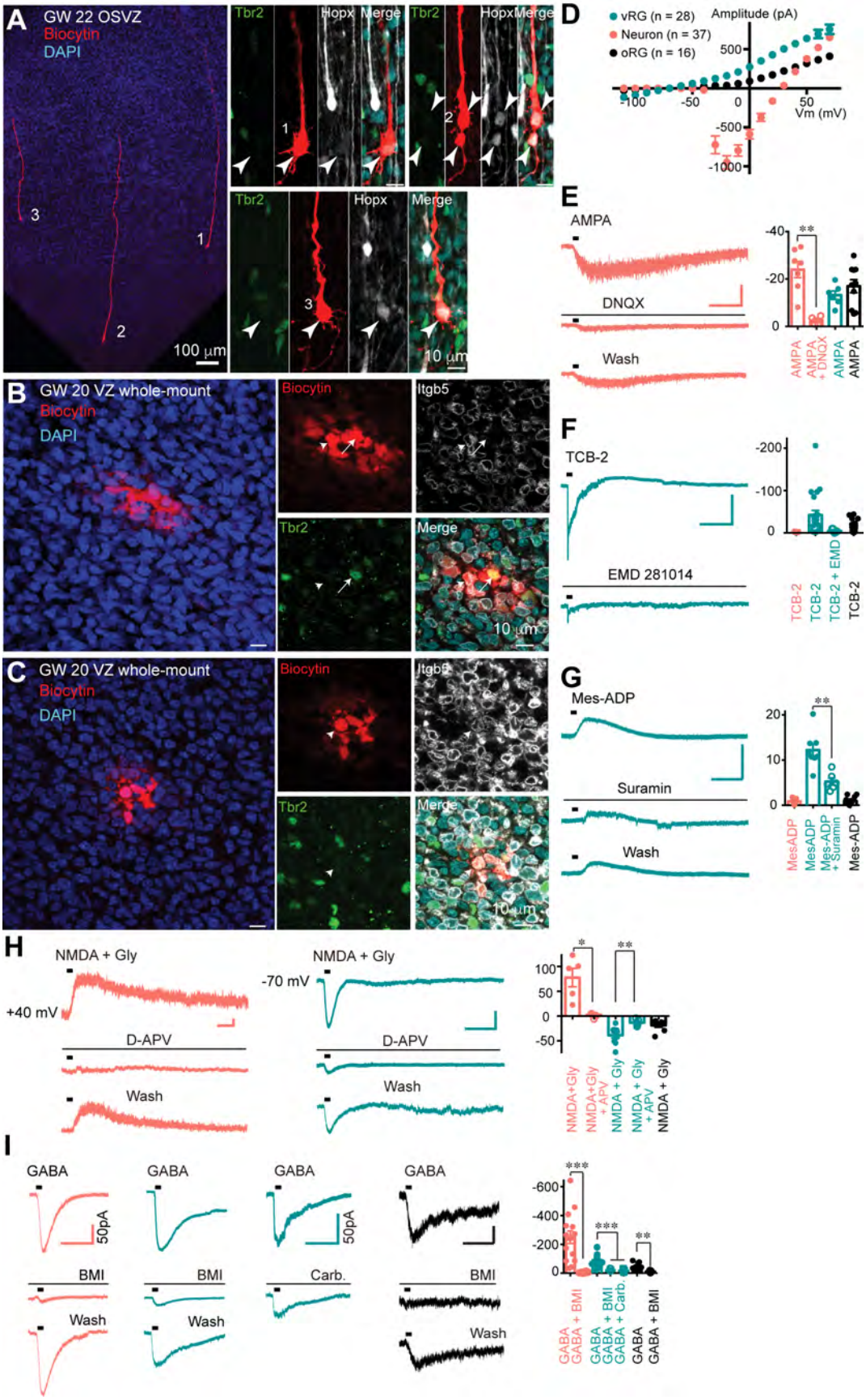
A
GW 22 OSVZ
Biocytin
DAPI
Tbr2
Hopx
Merge
100 μm
10 μm
B
GW 20 VZ whole-mount
Biocytin
DAPI
Itgb5
C
GW 20 VZ whole-mount
D
vRG (n = 28)
Neuron (n = 37)
oRG (n = 16)
Amplitude (pA)
Vm (mV)
E
AMPA
DNQX
Wash
F
TCB-2
EMD 281014
TCB-2 + EMD
G
Mes-ADP
Suramin
MesADP
Mes-ADP + Suramin
H
NMDA + Gly
+40 mV
-70 mV
D-APV
NMDA+Gly + APV
NMDA + Gly + APV
I
GABA
BMI
Carb.
50pA
GABA + BMI
GABA + BMI + Carb

Figure S2 Patch-clamp recordings and morphology reconstruction in acute slices of the developing human cortex, Related to Figure 2: (A) Morphology of oRG cells and vRG cells **(B,C)** labeled by biocytin and immunostained with cell type-specific markers. vRG cells were recorded and imaged from manually dissected whole-mount ventricular zone slices. **(D**) The current-voltage curve (I-V) of neurons, ventricular radial glia (vRGs) or outer radial glia (oRGs) recorded in the developing human cortex cortical plate or germinal zone. Peak currents were measured from voltage-gated currents obtained with a stepped voltage protocol. **(E)** Representative traces and statistical results show AMPA-induced inward current was reversibly blocked by DNQX (20 μM). **(F)** Representative traces and statistical analysis show TCB-2-induced inward current was blocked by EMD 281014 (200 μM). **(G)** Example traces and statistical analysis show MeSADP induced an outward current only in radial glia. The outward current was reversibly blocked by suramin (100 μM). **(H)** Representative traces and statistical results show NMDA plus glycine (Gly)-induced current was reversibly blocked by D-APV (100 μM). **(I**) Representative traces and statistical results show GABA-induced current was reversibly blocked by bicuculline (BMI, 20 μM). GABA-induced current in radial glia cells was decreased in the presence of gap junction blocker carbenoxolone (Carb. 100 μM) (One-way ANOVA, *** $P < 0.001$). Neurons (red traces) were held at -60 mV except for NMDA + Glycine (held at +40 mV). All oRGs (back traces) and vRGs (green traces) were recorded from cells held at -70 mV. (Paired t-test. * $P < 0.05$; ** $P < 0.01$; *** $P < 0.001$). Scale bars: 5 s and 20 pA unless otherwise noted.

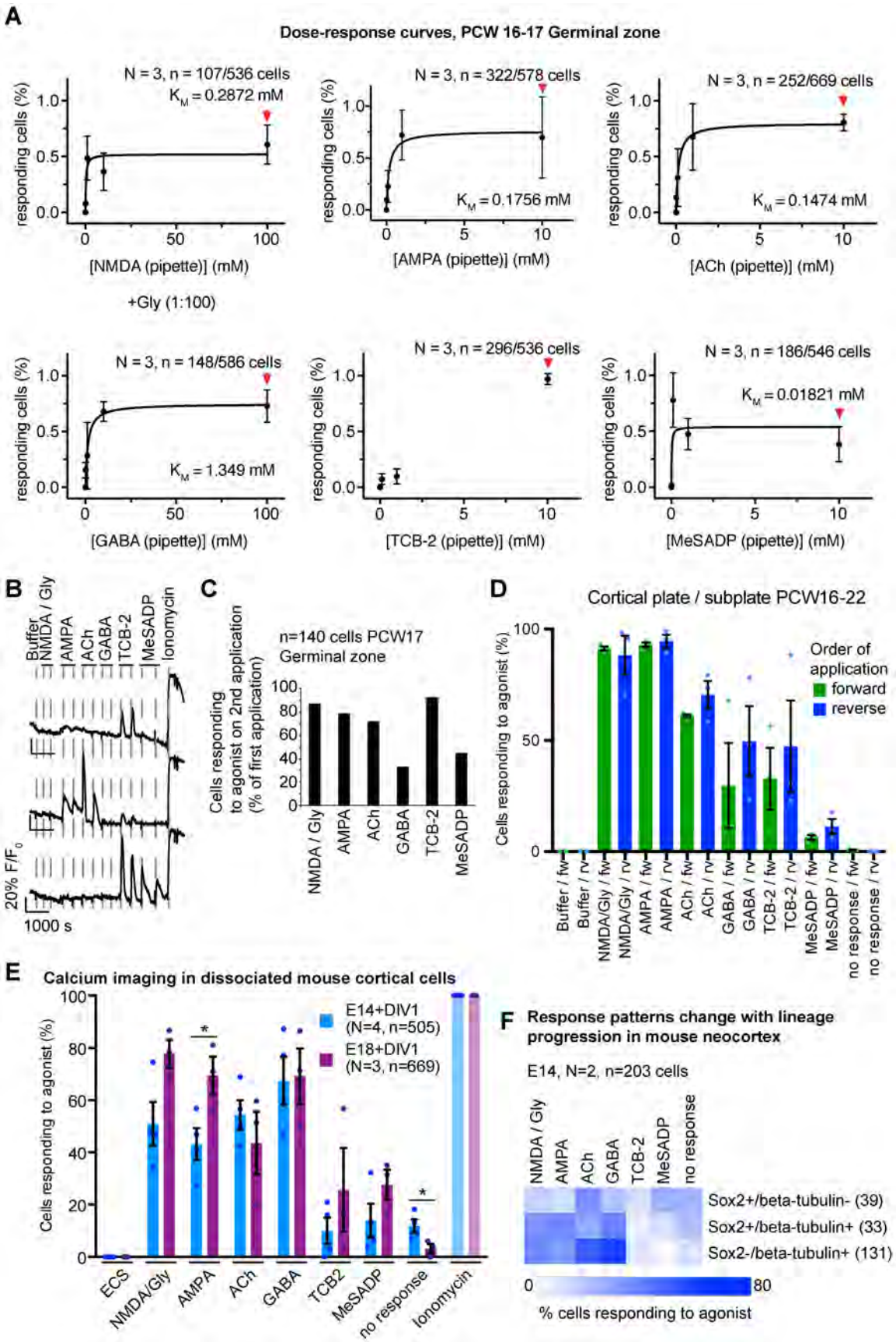
A
Dose-response curves, PCW 16-17 Germinal zone
N = 3, n = 107/536 cells
K_M = 0.2872 mM
responding cells (%)
[NMDA (pipette)] (mM)
+Gly (1:100)
N = 3, n = 322/578 cells
K_M = 0.1756 mM
[AMPA (pipette)] (mM)
N = 3, n = 252/669 cells
K_M = 0.1474 mM
[ACh (pipette)] (mM)
N = 3, n = 148/586 cells
K_M = 1.349 mM
[GABA (pipette)] (mM)
N = 3, n = 296/536 cells
[TCB-2 (pipette)] (mM)
N = 3, n = 186/546 cells
K_M = 0.01821 mM
[MeSADP (pipette)] (mM)
B
Buffer
NMDA / Gly
AMPA
ACh
GABA
TCB-2
MeSADP
Ionomycin
20% F/F0
1000 s
C
n=140 cells PCW17
Germinal zone
Cells responding to agonist on 2nd application (% of first application)
NMDA / Gly
AMPA
ACh
GABA
TCB-2
MeSADP
D
Cortical plate / subplate PCW16-22
Cells responding to agonist (%)
Order of application
forward
reverse
Buffer / fw
Buffer / rv
NMDA/Gly / fw
NMDA/Gly / rv
AMPA / fw
AMPA / rv
ACh / fw
ACh / rv
GABA / fw
GABA / rv
TCB-2 / fw
TCB-2 / rv
MeSADP / fw
MeSADP / rv
no response / fw
no response / rv
E
Calcium imaging in dissociated mouse cortical cells
Cells responding to agonist (%)
E14+DIV1
(N=4, n=505)
E18+DIV1
(N=3, n=669)
ECS
NMDA/Gly
AMPA
ACh
GABA
TCB2
MeSADP
no response
Ionomycin
F
Response patterns change with lineage progression in mouse neocortex
E14, N=2, n=203 cells
NMDA / Gly
AMPA
ACh
GABA
TCB-2
MeSADP
no response
Sox2+/beta-tubulin- (39)
Sox2+/beta-tubulin+ (33)
Sox2-/beta-tubulin+ (131)
% cells responding to agonist

Figure S3 Ca^{2+} imaging in bulk cell culture control experiments, Related to Figure 3: (A) Dose-response curves for the six different agonists used in this study were determined by Ca^{2+} imaging of dissociated cells from the germinal zone at GW 18-19. Curves were fitted using Michaelis-Menten kinetics, and the Michaelis constants (K_M) were determined. TCB-2 dose-response curve could not be fitted because saturation was not reached with the concentrations tested. For all further experiments a supersaturating concentration at least 10 fold higher than Km was used (denoted by red arrow). Note that TCB-2 is not soluble in an aqueous solution at higher concentrations. **(B)** Agonists were applied twice in a row in order to test for the robustness of the Ca^{2+} response. Three characteristic traces are shown from GW 19 germinal zone cells. **(C)** Bar graph shows percentage of cells responding to second application of agonist with respect to the first application. In most cases sequential application of the same agonist elicited a Ca^{2+} elevation in response to each agonist application. **(D)** Agonists were applied either in a forward (fw, green bars) or reverse (rv, blue bars) direction on dissociated cells from the CP/SP and responses were recorded by Ca^{2+} imaging. In the forward direction agonists were applied in the following order: NMDA/Gly, AMPA, ACh, GABA, TCB-2, MeSADP, Ionomycin. In the reverse order agonists were applied in the following order: MeSADP, TCB-2, GABA, ACh, AMPA, NMDA/Gly, Ionomycin. No significant differences were found between the two orders of agonist application. Mean ± SEM are indicated. **(E)** Calcium imaging in dissociated mouse cortical cells at E14 + Days in vitro (DIV) 1 and E18 + DIV1. Summarized results of the percentage of cells showed

Ca^{2+} elevation upon agonist stimulation. Statistical significance of changes between the two time points were determined using t-tests for each agonist, * $p<0.05$. Data are represented as mean ± SEM, dots indicate biological replicates **(F)** Immunocytochemistry after calcium imaging was performed to identify enrichment of responses in neurons (beta-tubulin-positive), progenitor cells (Sox2-positive), and newborn neurons (Sox2 and beta-tubulin-positive). Heatmap shows the percentage of each cell type responding to each of the agonists, number of cells per category shown in brackets.

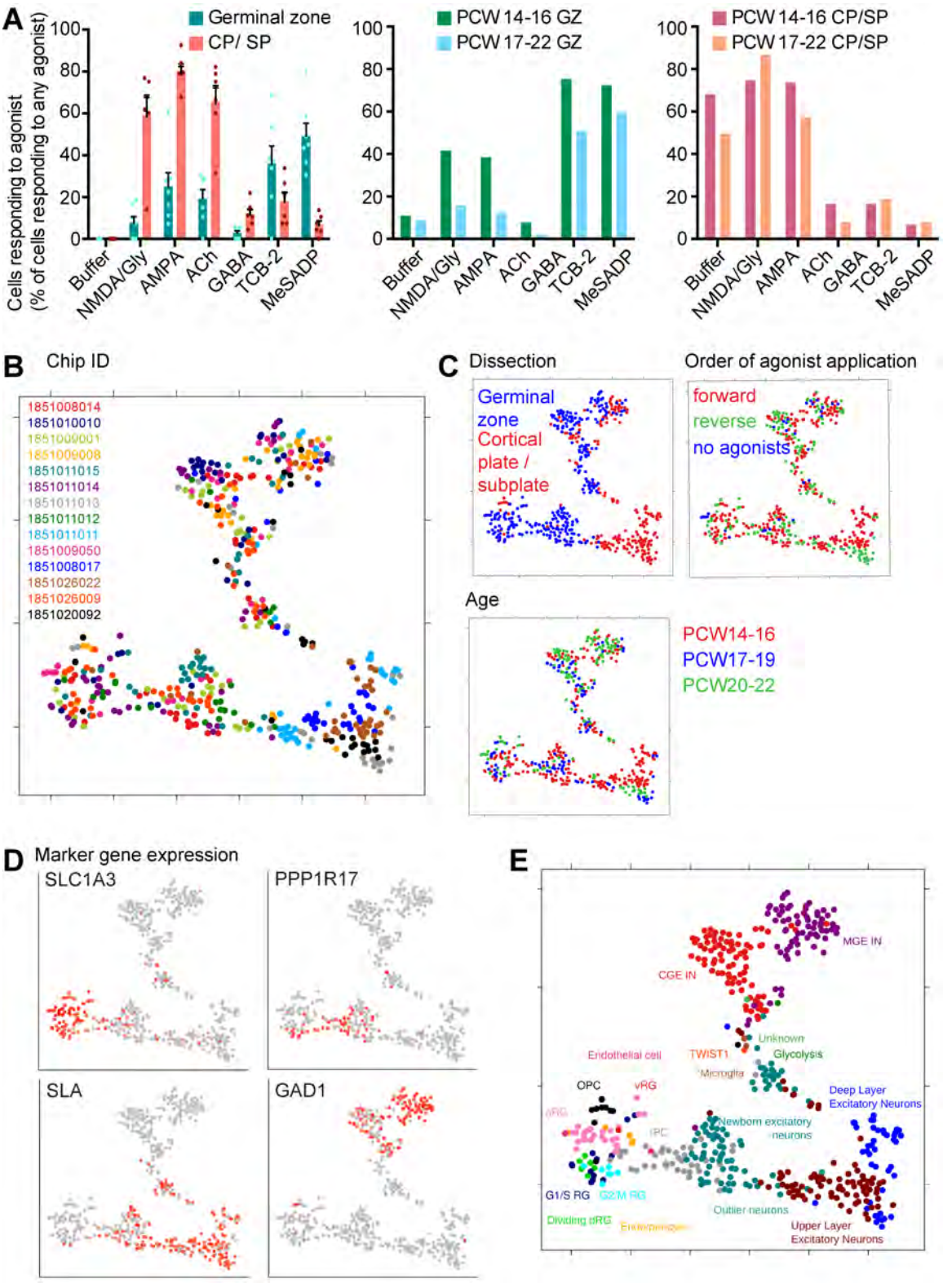
A
Cells responding to agonist
(% of cells responding to any agonist)
Germinal zone
CP/ SP
PCW 14-16 GZ
PCW 17-22 GZ
PCW 14-16 CP/SP
PCW 17-22 CP/SP
Buffer
NMDA/Gly
AMPA
ACh
GABA
TCB-2
MeSADP
B
Chip ID
1851008014
1851010010
1851009001
1851009008
1851011015
1851011014
1851011013
1851011012
1851011011
1851009050
1851008017
1851026022
1851026009
1851020092
C
Dissection
Germinal zone
Cortical plate / subplate
Order of agonist application
forward
reverse
no agonists
Age
PCW14-16
PCW17-19
PCW20-22
D
Marker gene expression
SLC1A3
PPP1R17
SLA
GAD1
E
MGE IN
CGE IN
Unknown
Endothelial cell
TWIST1
Glycolysis
Microglia
OPC
vRG
oRG
Deep Layer Excitatory Neurons
Newborn excitatory neurons
IPC
G1/S RG
G2/M RG
Outlier neurons
Dividing tRG
Endothelial
Upper Layer Excitatory Neurons

Figure S4 Polaris single-cell capture metadata, Related to Figure 4: (A) Population Ca^{2+} responses of cells captured on Polaris microfluidic chips. Note that the relative responses to each one of the agonists are similar to the percentage responses in bulk culture (Figure 3D, F, G). **(B)** Feature plot of cells captured on Polaris microfluidic chips (Figure 4D) and colored based on Polaris microfluidic chip ID, see Table S2 for metadata. **(C)** Feature plot of cells captured on Polaris microfluidic chips (Figure 4D) and colored based on the laminar dissection, the order of agonist application (forward: NMDA/Gly, AMPA, ACh, GABA, TCB-2, MeSADP, reverse is the opposite order, or no agonist dosing), or the age of the tissue. **(D)** Feature plot of cells captured on Polaris microfluidic chips (Figure 4D) colored based on the expression of marker genes. **(E)** Feature plot of cells captured on Polaris microfluidic chips (Figure 4D) colored based on the assignment of clusters after co-clustering with the C1 data (Figure 4F).

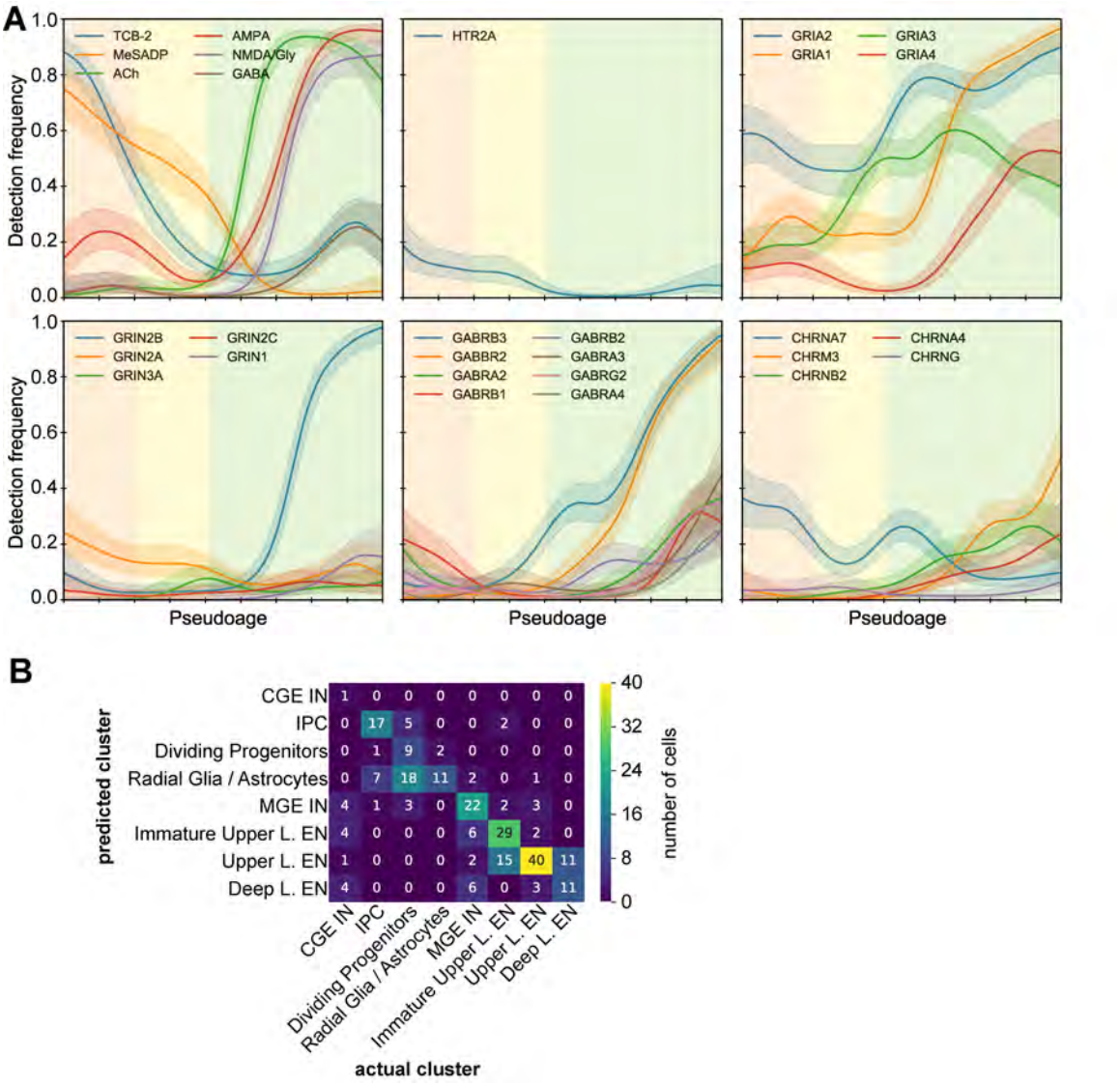

Figure S5 Correlation of receptor expression, physiological responses, and cell types, Related to Figure 6: (A) The frequency of responses to agonist application varies as a function of pseudoage and is correlated to expression of specific receptor subunits. Detection frequencies of agonist responses and receptor genes (for receptors expressed in more than 5 cells) in pseudoage are shown. **(B)** Confusion matrix showing physiologically predicted cluster vs. transcriptomically identified cluster in the training data. Heatmap showing the

number of cells of a transcriptomically identified cluster that where classified as belonging to a particular cluster. The good classification accuracy is present as the high counts along the diagonal. The misclassifications (off-diagonal entries) mainly occur between related cell types due to their more similar response patterns.

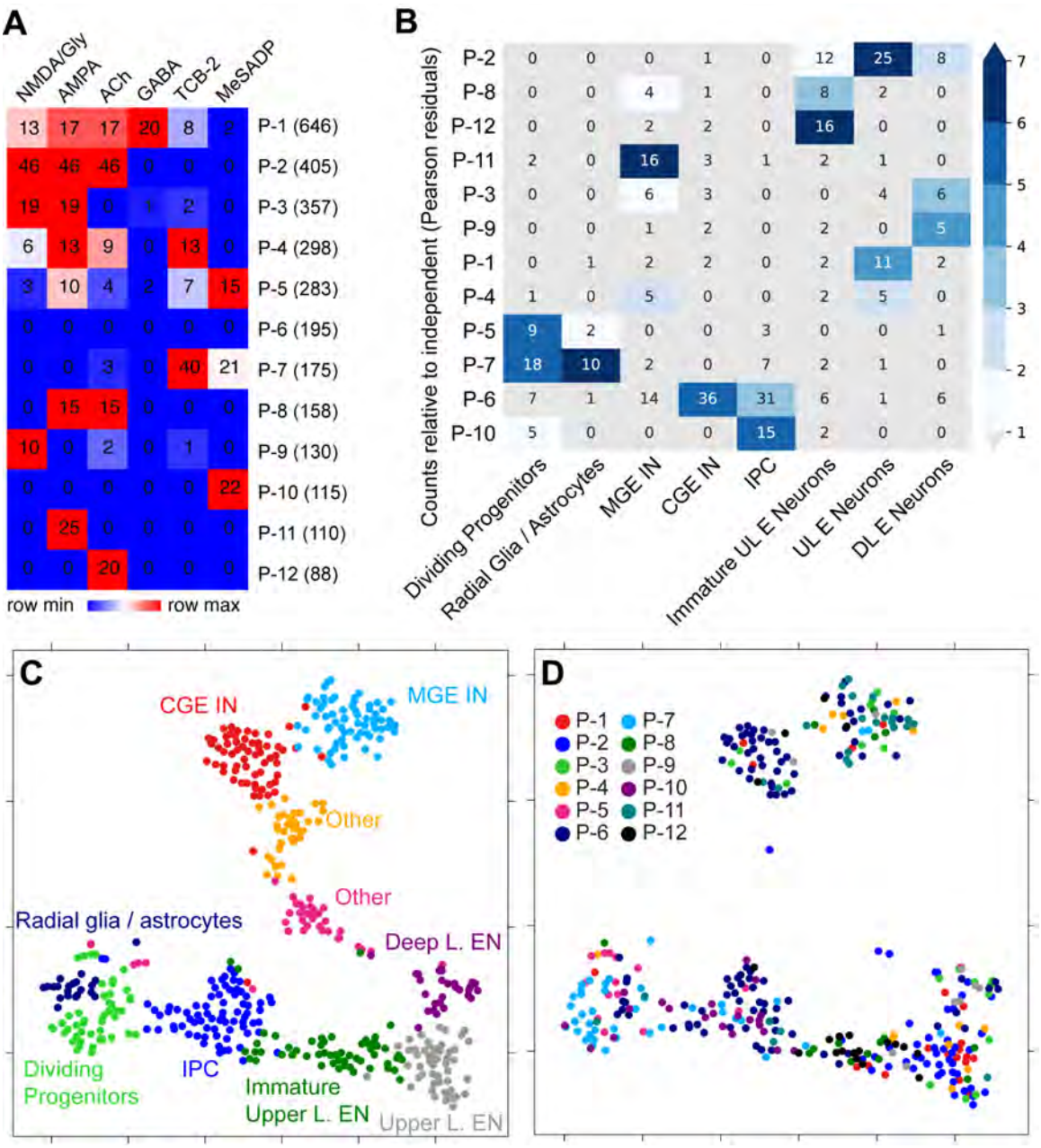

Figure S6 Mapping physiological response types onto molecular clusters, Related to Figure 7: (A) Heatmap showing the relative responses to each neurotransmitter (columns) in the different physiological types (P, rows). Numbers in brackets indicate total number of cell in the cluster (combined from the bulk experiments and the microfluidic single-cell experiments). Numbers in

the heat map indicate number of cells in each cluster analyzed on microfluidic chips at the single-cell level. (**B)** Hierarchical clustering of physiological types (P, rows) and molecularly defined cell types (columns) in a contingency table (Figure 3C) using Pearson residuals. **(C)** Feature plot of cells captured on Polaris microfluidic chips with cell type assignment (Figure 4D). **(D)** Feature plot of cells captured on Polaris microfluidic chips (A) and colored based on the physiological type (P1-P12). **(E)** BrdU incorporation is not changed after TCB-2 stimulation in cortical slices. Slices were incubated in the presence of BrdU and specific agonists and antagonists for 24 hours, subsequent immunohistochemistry revealed no change in the proportion of proliferating cells as indicated by Ki67 staining and BrdU incorporation.